

GARDNet: Robust Multi-View Network for Glaucoma Classification in Color Fundus Images

Ahmed Al Mahrooqi*, Dmitrii Medvedev*, Rand Muhtaseb*, and Mohammad Yaqub

Mohamed bin Zayed University of Artificial Intelligence
Abu Dhabi, UAE

{ahmed.mahrooqi, mohammad.yaqub}@mbzuai.ac.ae

Abstract. Glaucoma is one of the most severe eye diseases, characterized by rapid progression and leading to irreversible blindness. It is often the case that diagnostics is carried out when one’s sight has already significantly degraded due to the lack of noticeable symptoms at early stage of the disease. Regular glaucoma screenings of the population shall improve early-stage detection, however the desirable frequency of etymological checkups is often not feasible due to the excessive load imposed by manual diagnostics on limited number of specialists. Considering the basic methodology to detect glaucoma is to analyze fundus images for the *optic-disc-to-optic-cup ratio*, Machine Learning algorithms can offer sophisticated methods for image processing and classification. In our work, we propose an advanced image pre-processing technique combined with a multi-view network of deep classification models to categorize glaucoma. Our *Glaucoma Automated Retinal Detection Network (GARDNet)* has been successfully tested on Rotterdam EyePACS AIROGS dataset with an AUC of 0.92, and then additionally fine-tuned and tested on RIM-ONE DL dataset with an AUC of 0.9308 outperforming the state-of-the-art of 0.9272. Our code will be made available on GitHub upon acceptance.

Keywords: Glaucoma Classification · Color Fundus Images · Computer Aided Diagnosis.

1 Introduction

Glaucoma is an eye disease which is considered the leading cause of blindness. It is caused by an increased pressure in the eyes as a result of fluid build up, clinically known as *intraocular pressure (IOP)*, which damages the optic nerve. Patients with glaucoma do not usually experience apparent symptoms, as such, it is referred to as the “silent thief of sight” [9]. A study by Ronan Conlon et al. [2] projected 80 million cases of glaucoma worldwide by the year 2020.

Another recent study reported that by the year 2040, 111.8 million people will be affected by this disease [1]. Among many types of glaucoma, there are

* Equal contribution.

two common types, specified by the structural nature of the disease: *angle closure glaucoma (ACG)* and *open angle glaucoma (OAG)*. The former type is more common, while the latter progresses much faster to complete blindness with no early intervention. While measuring the IOP may sometimes help clinicians in diagnosis, it is difficult to accurately take readings due to the unstable nature of optical pressure. Clinicians have resorted to examining the structure and appearance of *optic disc (OD)*, such as the increase of the *cup-to-disc ratio (CDR)* [9]: the ratio of the optic cup diameter to the diameter of the OD. However, manual examination is time-consuming operation and is a subject to the availability of a specialist. In order to release ophthalmologists from the burden of manual glaucoma screening, multiple automated approaches involving deep learning techniques are explored.

In this paper, we propose *Glaucoma Automated Retinal Detection Network (GARDNet)*: a combined methodology of sophisticated image pre-processing and robust multi-view network architecture for glaucoma classification. Our model was trained and tested on AIROGS training dataset [18] which has images of different quality and resolution. In order for our model to produce consistent and robust results regardless of the aforesaid conditions, we introduced a localization of the area of interest with the following pre-processing pipeline. GARDNet extracts bounding boxes around the OD, and then applies multiple random affine and non-linear transformations, as well as such image processing techniques as *Contrast Limited Adaptive Histogram Equalization (CLAHE)*. Overall, we have validated eight models with over 150 experiments, and combined three best performing models in a multi-view network manner. Our proposed methodology allowed us to achieve AUC of 0.9308 on an external testing dataset, outperforming the state-of-the-art model by Fumero et al. [6] which achieved 0.9272 on the same dataset. This work does not aim to propose a new algorithm nor expand on an existing one. We aim to propose and validate a robust solution for glaucoma classification.

2 Related Works

Glaucoma related research is mainly focused on automated methods of disease screening and segmentation of the OD and its outer area, with the following classification of referable/no-referable glaucoma. For example, Dibia et al. in [3] proposed to extract from segmented OD such features of eye fundus images as optic disc area, cup diameter, rim area and other important features to calculate *then Cup-to-disc ratio (CDR)*, which is commonly used as an indicator of glaucoma. Although the proposed methodology has a strong logical foundation, it was tested on a rather small dataset. Furthermore, many research papers introduce deep-learning based methods to classify glaucoma. Lee et al. in [10] proposed fully automated CNN, called M-Net, based on a modified U-Net [13] to segment OD and *optic cup (OC)*. For the glaucoma classification task, the team used pretrained ResNet50 and affine transformations for image preprocessing, achieving AUC of 0.96 on the small dataset, REFUGE [5]. Similar approach of

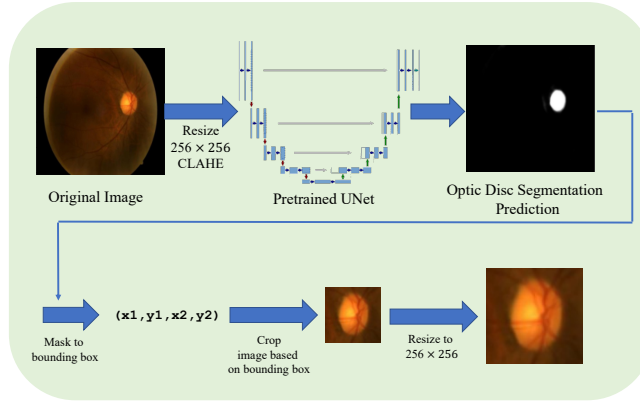


Fig. 1. Preprocessing pipeline used in our experiments on the AIROGS dataset to crop the regions of interest from the original images.

two-step glaucoma screening was presented by Sreng et al. [17], suggesting to segment OD using DeepLabV3, and then classify glaucoma using various deep CNNs such as AlexNet, GoogleNet, and InceptionV3 among others. The authors worked with several datasets and achieved promising results, but faced some limitations when attempting to generalize between datasets. Maadi et al. in [11] followed the same segment-and-classify approach. As a novelty, the authors modified classical U-Net model, introducing pre-trained SE-ResNet50 on the encoding layers which achieved better results. In a more recent work, Phasuk et al. in [12], proposed improvements of *disc-aware ensemble network (DENet)* which incorporates the information from general fundus image with the information from optic disc area. This allowed the authors to achieve AUC of 0.94 on a combined testing set from RIM-ONE-R3 [8] and Drishti-GS [16].

3 Method

3.1 Preprocessing

The AIROGS dataset [18] used in our experiments have non-uniform dimensions. We therefore begin by resizing all images to a fixed dimension of 256×256 pixels. In addition, we apply CLAHE transformation, and then feed our resized images to a U-Net model [13] pretrained on optic disc segmentation [15] using the RIM-ONE v3 dataset [7]. The generated optic disc segmentation masks are then converted to bounding box coordinates, with padding determined by taking 30% of the segmented optic disc’s diameter. We then proceed with cropping the original image based on the values of the bounding box coordinates, and finally resize the cropped image to a uniform dimension of 256×256 pixels. In the case where the pretrained network fails to segment the optic disc, we default by taking a center crop of size 85% of the image width, followed by a resize to

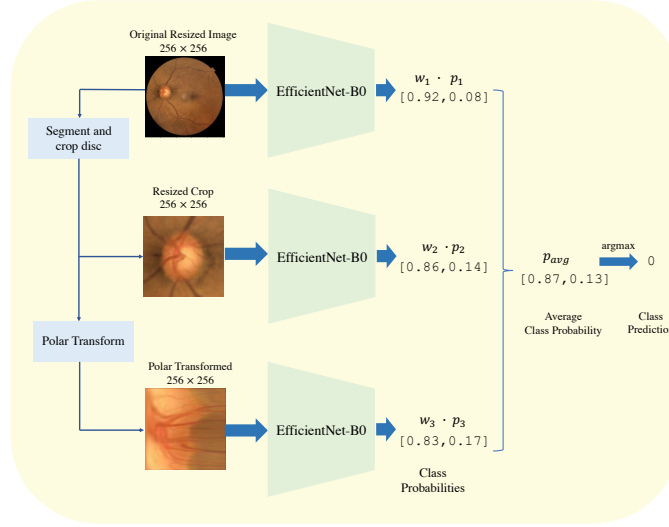


Fig. 2. Our multi-view network is composed of three different CNNs trained on different views of the color fundus images. The classification result is obtained by a weighted averaging of the class probabilities in each model. w_n refers to the weight coefficient corresponding to model n , and p_n is the soft-max probability predictions in model n .

256×256 pixels. This accounts for approximately 20% of our dataset. Figure 1 illustrates our overall preprocessing pipeline.

3.2 Multi-View Classification Network

Our glaucoma classification model, GARDNet, is composed of a multi-view network of three different convolutional neural networks (CNNs) trained on different views of the color fundus images, as illustrated in Figure 2. The first network is trained on the original resized images, whereas the second network is trained on the cropped disc area generated from the preprocessing step, and finally, the third network is trained on the polar transformed cropped images. The training of each model is done independently. The model choice in the final multi-view network is based on ablation studies using different architectures, as reported in later sections. The intuition behind the multi-view network is that, experimentally, the model with uncropped images performed better than the cropped images. This is likely due to the error introduced by the pretrained disc segmentation model that is used to crop the images. At the same time, cropped images containing the optic disc area are most important for glaucoma diagnosis, as stated in the literature [10] and shown experimentally in our GradCAM [14] visualization Figure 3. We therefore retain both models in the final multi-view network. Lastly, in the final model, we apply polar transformation, which converts the image representation from Cartesian coordinates to polar coordinates

system. For a point (u, v) in the Cartesian space, we obtain the radius r and angle θ as follows [4]:

$$\begin{cases} r = \sqrt{u^2 + v^2} \\ \theta = \tan^{-1}(\frac{v}{u}) \end{cases} \leftrightarrow \begin{cases} u = r \cos \theta \\ v = r \sin \theta \end{cases} \quad (1)$$

The transformation converts the radial relationship between the optic disc, cup, and background to a spatial hierarchical structure, which may provide an alternative view to the classification model and help capture more complex features. Phasuk et al. [12] claims that this transformation enhances the low level information in the optic disc region. The final classification prediction is obtained by taking a weighted average of the three soft-max predictions, followed by assigning the prediction label to the class that scored the highest probability. In the final multi-view network, we assign higher weight ($w = 2$) to the model trained on uncropped images, as it performed better on the validation set. The other two models generally performed similarly and therefore share the same weight.

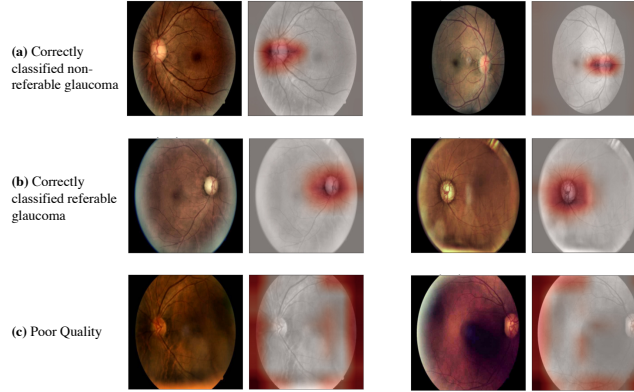


Fig. 3. GradCAM [14] visualization on EfficientNet-B0 model trained on the uncropped AIROGS dataset.

4 Datasets

Rotterdam EyePACS AIROGS The Rotterdam EyePACS AIROGS dataset [18] consists of 113,893 color fundus images. The training set is only available to be downloaded, which has 101,442 gradable images (images of acceptable quality). The testing set consists of 11,000 gradable and ungradable images but it is not accessible to the public which limited our ability to use in this paper. Each image in the dataset is annotated by an expert as “referable glaucoma” or “no referable glaucoma”. The images are high in resolution and do vary in

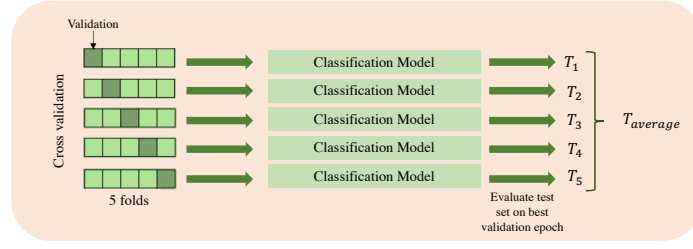


Fig. 4. 5-fold cross-validation applied on our dataset, where T_n is the test results evaluated using the model trained on fold n and $T_{average}$ is the average test results across all $k=5$ folds.

size. The dataset has significant class imbalance, where the size of “no referable glaucoma” (normal) class is approximately 15 times greater than the “referable glaucoma” class.

RIM-ONE DL Retinal Image database for Optic Nerve Evaluation for Deep Learning (RIM-ONE DL) dataset [6] is used in this project as an external testing dataset, which consists of 313 normal and 172 glaucomatous fundus images. All images were segmented, then cropped around the cup-disc area. There are two training/testing split versions of this dataset; one was split randomly and the other was split by hospitals in Madrid and Zaragoza. We chose to report the results on the one split by the hospitals. The training set consists of 311 images, and the testing set contains 174 images.

5 Experimental Setup

For the following datasets, all the images were resized to 256×256 . To address the problem of the imbalanced classes in both datasets, we utilize weighted cross entropy as a loss function. The evaluation metrics used are Area Under Curve (AUC) and F-score (F1).

Rotterdam EyePACS AIROGS Our models were trained for 50 epochs on a single NVIDIA A100 GPU with a batch size of 64. An Adam optimizer was used with a learning rate ranging between 1×10^{-4} - 1×10^{-3} . For some experiments, we apply data augmentations consisting of random vertical flip ($p = 0.5$), random horizontal flip ($p = 0.5$) and random rotation (degrees= $(-10^\circ, +10^\circ)$). In some experiments, we apply CLAHE transformation, as inspired by previous works. The advantage of using CLAHE is that it enhances the contrasts and dampens any noise amplification [12]. Given that the original testing set is not available, we split the training data into training and testing splits, using approximately 90/10 percents. To validate the robustness of our models, we performed 5-fold cross-validation by splitting the training data into training and validation,

with approximately 80/20 percent, as illustrated in Figure 4. As a result, the dataset sizes for training, validation, and testing are 73,154, 18,288 and 10,000, respectively.

RIM-ONE DL For this dataset, our main goal is to validate our model trained on the Rotterdam EyePACS AIROGS generalizability on a completely new unseen dataset. We visually noticed that the optic disc occupied a larger area in the image. We therefore retrain our best model with scaling augmentation that mimics this behavior, and results in a model invariant to images with different scales. We fine-tuned our pretrained models using dropout rate of 0.2, learning rate of 5×10^{-3} and augmentations such as random horizontal and vertical flips as well as scaling. Since the RIM-ONE DL dataset is already cropped around the optic disc (OD) area, our multi-view network for this experiment consisted of only two models, while ignoring the model trained on original uncropped images. This makes our proposed solution applicable to different datasets with varying sizes and crops.

6 Experiments & Results

Rotterdam EyePACS AIROGS Table 1 shows a summary of our experiments on the Rotterdam EyePACS AIROGS dataset. On the cropped data, we performed multiple experiments using different convolutional neural networks such as EfficinetNet-B0, EfficinetNet-B1, MobileNet-V3, ResNet18, ResNet34, ResNet50 and DenseNet in addition to Vision Transformer (ViT-Base) with patch size 16. We experimented with several experimental hyperparameters such as dropout, applying CLAHE and augmentations. Our best performance on the cropped images was obtained with EfficientNet-B0 model with dropout ($p = 0.5$), CLAHE and augmentations, gaining an AUC of 0.90 ± 0.01 and F1-score of 0.77 ± 0.01 . To verify the performance of our cropped images vs. the original images, we trained the original images on the same model configurations as our best model, and obtained a higher AUC of 0.91 ± 0.01 and F1-score of 0.79 ± 0.01 . Additionally, we further repeated the training of the best scoring model using polar transformations, which obtained a slightly inferior performance of AUC 0.85 ± 0.02 and F1-score of 0.76 ± 0.01 .

RIM-ONE DL Table 2 summarizes our testing results on the RIM-ONE DL dataset after fine-tuning our pretrained models (Experiment #10 and #14) on the RIM-ONE DL training split. As shown in Table 2, our multi-view network achieves a better performance compared to [6], obtaining an AUC of 0.9308 and F1-Score of 0.9170. The individual CNNs corresponding to Experiments #10 and #14 obtained an inferior performance of AUC 0.87954 and 0.9088 respectively.

Table 1. Experimental results on the Rotterdam EyePACS AIROGS dataset. D =dropout, A =augmentations, C =CLAHE, S =scaling transformation, P =polar transformation. EfficientNet-B0_{original} refers to EfficientNet-B0 model trained on the original (uncropped) data.

ID	Model	Test AUC	Test F-1
1	Resnet34	0.74 ± 0.02	0.74 ± 0.01
2	Resnet18	0.75 ± 0.02	0.74 ± 0.01
3	Resnet34 (C)	0.78 ± 0.01	0.75 ± 0.01
4	ViT-B $_{224 \times 224}$	0.78 ± 0.01	0.75 ± 0.01
5	DenseNet-121	0.79 ± 0.04	0.71 ± 0.06
6	MobileNet-V3 Large	0.79 ± 0.02	0.78 ± 0.00
7	EfficientNet-B1	0.81 ± 0.02	0.80 ± 0.01
8	EfficientNet-B0	0.81 ± 0.02	0.79 ± 0.01
9	Resnet50	0.82 ± 0.02	0.80 ± 0.00
10	EfficientNet-B0 (D,A,C,P)	0.85 ± 0.02	0.76 ± 0.01
11	EfficientNet-B0 (A,C)	0.87 ± 0.01	0.80 ± 0.01
12	MobileNet-V3 Large (D,A,C)	0.89 ± 0.01	0.77 ± 0.01
13	EfficientNet-B0 (D,A,C,S)	0.89 ± 0.01	0.76 ± 0.01
14	EfficientNet-B0 (D,A,C)	0.90 ± 0.01	0.77 ± 0.01
15	EfficientNet-B0 _{original} (D,A,C)	0.91 ± 0.01	0.79 ± 0.01
16	Multi-view network (#10, #14, #15)	0.92	0.80

Table 2. Experimental results on RIM-One DL dataset.

Model	Test AUC	Test F-1
Fumero et al. [6]	0.9272	-
Experiment #10 (Ours)	0.8795	0.8517
Experiment #14 (Ours)	0.9088	0.8974
Multi-view network (#10, #14) (Ours)	0.9308	0.9170

7 Discussion

Our results indicate that the models trained on the uncropped images performed much better than the cropped images. We hypothesize that this is due to errors introduced by the pretrained disc segmentation model that is used to crop the images. Furthermore, our experiments show that using dropout improves the performance, and therefore is a good strategy for overfitting. Additionally, using augmentations and CLAHE on top of dropout significantly improves the performance. By using augmentations and CLAHE, we increase the effective dataset size and also overcome model overfitting, making it robust to spatial and color transformations.

Furthermore, the ViT-B model did not perform as good as the EfficientNet-B0 model. The Vision Transformer model requires a large amount of data to perform as well as CNNs, therefore we hypothesize that its inferior performance is probably due to the relatively small number of training samples. In addition,

ResNet18 and ResNet34 models performed worse, as smaller models are not able to capture the complex features in our dataset.

The multi-view network outperformed all previous experiments in the AIROGS dataset. By combining our three best performing CNNs, each trained on a different view of the same data, we achieve an AUC of 0.92. Furthermore, we give more classification decision weight to the best performing CNN, Experiment #15 (Table 1), which helped achieve this performance.

For the RIM-ONE DL experiments, we can conclude that our multi-view network, GARDNet, generalizes well on this dataset when fine-tuned on the training set. While experiment #10 and #14 did not exceed in performance compared to the previous state-of-the-art, the multi-view network composed of these two models scored a higher AUC score than Fumero et al. [6]. We hypothesize that our model performed better due to our image processing methods such as CLAHE and polar transformations, as well as the availability of a large dataset for pretraining. Furthermore, as our results indicate, multi-view networks outperform individual models.

8 Conclusion

In this paper, we introduced a multi-view network GARDNet for glaucoma classification composed of three different CNNs trained on different views of the color fundus images. We trained our model on the AIROGS dataset and tested our results on a subset of that dataset in addition to an external dataset, RIM-ONE DL. Our results indicate that the multi-view network significantly improves the performance when compared to individual models. Furthermore, when testing our data on the external dataset, we get superior performance to the previous state of the art model by Fumero et al. [6] after fine-tuning the model. In future works, we would like to extend the weighted averaging of the multi-view network predictions, such that the weights are determined systematically rather than being constant. Additionally, we would like to evaluate the performance of GARDNet using smaller fractions of the training dataset, to understand the impact of dataset size to our model performance.

References

1. Allison, K., Patel, D., Alabi, O.: Epidemiology of Glaucoma: The Past, Present, and Predictions for the Future. *Cureus* (Nov 2020). <https://doi.org/10.7759/cureus.11686>, <https://www.cureus.com/articles/42672-epidemiology-of-glaucoma-the-past-present-and-predictions-for-the-future>
2. Conlon, R., Saheb, H., Ahmed, I.I.K.: Glaucoma treatment trends: a review. *Canadian Journal of Ophthalmology* **52**(1), 114–124 (Feb 2017). <https://doi.org/10.1016/j.jcjo.2016.07.013>, <https://linkinghub.elsevier.com/retrieve/pii/S0008418216300758>
3. Dibia, A.C., Nwawudu, S.E.: Automated detection of glaucoma from retinal images using image processing techniques **7**, 2321–9009 (09 2018)
4. Fu, H., Cheng, J., Xu, Y., Wong, D.W.K., Liu, J., Cao, X.: Joint optic disc and cup segmentation based on multi-label deep network and polar transformation. *IEEE Transactions on Medical Imaging* **37**(7), 1597–1605 (jul 2018). <https://doi.org/10.1109/tmi.2018.2791488>, <https://doi.org/10.1109%2Ftmi.2018.2791488>
5. Fu, H., Li, F., Orlando, J.I., Bogunović, H., Sun, X., Liao, J., Xu, Y., Zhang, S., Zhang, X.: Refuge: Retinal fundus glaucoma challenge (2019). <https://doi.org/10.21227/tz6e-r977>, <https://dx.doi.org/10.21227/tz6e-r977>
6. Fumero, F., Diaz-Aleman, T., Sigut, J., Alayón, S., Arnay, R., Angel-Pereira, D.: Rim-one dl: A unified retinal image database for assessing glaucoma using deep learning. *Image Analysis and Stereology* **39** (10 2020). <https://doi.org/10.5566/ias.2346>
7. Fumero, F., Sigut, J., Alayón, Silvia andGonzález-Hernández, M., González de la Rosa, M.: Interactive tool and database for optic disc and cup segmentation of stereo and monocular retinal fundus images (06 2015)
8. Fumero, F., Sigut, J., Alayón, Silvia andGonzález-Hernández, M., González de la Rosa, M.: Interactive tool and database for optic disc and cupsegmentation of stereo and monocular retinal fundus images (06 2015)
9. Lee, D.A., Higginbotham, E.J.: Glaucoma and its treatment: A review. *American Journal of Health-System Pharmacy* **62**(7), 691–699 (Apr 2005). <https://doi.org/10.1093/ajhp/62.7.691>, <https://academic.oup.com/ajhp/article/62/7/691/5134357>
10. Lee, J., Lee, J., Song, H., Lee, C.: Development of an end-to-end deep learning system for glaucoma screening using color fundus images. *JAMA Ophthalmol.* **137**, 1353–1360 (2019)
11. Maadi, F., Faraji, N., Bibalan, M.H.: A Robust Glaucoma Screening Method for Fundus Images Using Deep Learning Technique. In: 2020 27th National and 5th International Iranian Conference on Biomedical Engineering (ICBME). pp. 289–293. IEEE, Tehran, Iran (Nov 2020). <https://doi.org/10.1109/ICBME51989.2020.9319434>, <https://ieeexplore.ieee.org/document/9319434/>
12. Phasuk, S., Poopresert, P., Yaemsuk, A., Suvannachart, P., Itthipanichpong, R., Chansangpetch, S., Manassakorn, A., Tantisevi, V., Rojanapongpun, P., Tantibundhit, C.: Automated glaucoma screening from retinal fundus image using deep learning. In: 2019 41st Annual International Conference of the IEEE Engineering in Medicine and Biology Society (EMBC). pp. 904–907 (2019). <https://doi.org/10.1109/EMBC.2019.8857136>
13. Ronneberger, O., Fischer, P., Brox, T.: U-net: Convolutional networks for biomedical image segmentation (2015). <https://doi.org/10.48550/ARXIV.1505.04597>, <https://arxiv.org/abs/1505.04597>

14. Selvaraju, R.R., Das, A., Vedantam, R., Cogswell, M., Parikh, D., Batra, D.: Grad-cam: Why did you say that? visual explanations from deep networks via gradient-based localization. CoRR **abs/1610.02391** (2016), <http://arxiv.org/abs/1610.02391>
15. Sevastopolsky, A.: Optic disc and cup segmentation methods for glaucoma detection with modification of u-net convolutional neural network. Pattern Recognition and Image Analysis **27**(3), 618–624 (jul 2017). <https://doi.org/10.1134/s1054661817030269>, <https://doi.org/10.1134/2Fs1054661817030269>
16. Sivaswamy, J., Krishnadas, S.R., Datt Joshi, G., Jain, M., Syed Tabish, A.U.: Drishti-gs: Retinal image dataset for optic nerve head(onh) segmentation. In: 2014 IEEE 11th International Symposium on Biomedical Imaging (ISBI). pp. 53–56 (2014). <https://doi.org/10.1109/ISBI.2014.6867807>
17. Sreng, S., Maneerat, N., Hamamoto, K., Win, K.Y.: Deep Learning for Optic Disc Segmentation and Glaucoma Diagnosis on Retinal Images. Applied Sciences **10**(14), 4916 (Jul 2020). <https://doi.org/10.3390/app10144916>, <https://www.mdpi.com/2076-3417/10/14/4916>
18. Coen de Vente, Koenraad A. Verrmeer, N.J.: Airogs: Artificial intelligence for robust glaucoma screening challenge. In: IEEE International Symposium on Biomedical Imaging. Ieee (2022)